Journal of Solid State Chemistry 205 (2013) 160–164

Contents lists available at ScienceDirect

Journal of Solid State Chemistry

journal homepage: www.elsevier.com/locate/jssc

# Nitrogen-tuned bonding mechanism of Li and Ti adatom embedded graphene

Sangho Lee, Yong-Chae Chung*

*Department of Materials Science and Engineering, Hanyang University, Seoul 133-791, Republic of Korea*

A R T I C L E  I N F O

*Article history:*
Received 13 May 2013
Received in revised form
28 June 2013
Accepted 3 July 2013
Available online 24 July 2013

*Keywords:*
N-doped grapheme
Bonding mechanism
Metal–graphene
DFT based ab-initio calculations

A B S T R A C T

The effects of nitrogen defects on the bonding mechanism and resultant binding energy between the metal and graphene layer were investigated using density functional theory (DFT) calculations. For the graphitic N-doped graphene, Li adatom exhibited ionic bonding character, while Ti adatom showed features of covalent bonding similar to that of pristine graphene. However, in the cases of pyridinic and pyrrolic structures, partially covalent bonding characteristic occurred around N atoms in the process of binding with metals, and this particular bond formation enhanced the bond strength of metal on the graphene layer as much as it exceeded the cohesive energy of the metal bulk. Thus, Li and Ti metals are expected to be dispersed with atomic accuracy on the pyridinic and pyrrolic N-doped graphene layers. These results demonstrate that the bonding mechanism of metal–graphene complex can change according to the type of N defect, and this also affects the binding results.

## 1. Introduction

Graphene, a single-atom thick carbon nanosheet, has emerged as a versatile material with distinctive properties originating from its two-dimensional (2D) honeycomb lattice [1–4]. Using these unique characteristics, a wide range of technical applications have been explored from conventional electronic devices to newly suggested energy materials [5–7]. One area of research, graphene in contact with metals is expected to broaden possible applications due to the combination of the high chemical property of metal atoms and the large surface areas of graphene. Therefore, there have been many theoretical and experimental attempts to apply metal embedded graphene to gas storage or sensing materials, catalysts, biodevices, and other applications [8–13].

However, there is a major obstacle using metal–graphene complex since metal atoms prefer to aggregate easily [14–15]. Under ambient conditions, dispersed metal atoms have a tendency to cluster because the cohesive energy of the metal itself is higher than the binding energy of the metal on the graphene. This unintended agglomerate has the effect of reducing the performance of devices using metal embedded graphene. For example, it was reported that the Li cluster formation on the graphene deteriorates the charge/discharge capacity of a battery when the graphene is used as anode materials for Li ion batteries [16]. Also, Sun et al. demonstrated that strong metal cohesion greatly decreases the weight percentage of hydrogen storage on metal functionalized carbon nanostructures [14]. Moreover, since high dimensional systems are known to cause degradation of the magnetic property, metal clustering hinders the application of metal–graphene complex to spintronic devices [17].

As a way to avoid this problem, surface modification of graphene by nitrogen doping has been suggested [18–19]. In recent years, several studies have shown that doping graphene with nitrogen is effective to tailor its electronic and magnetic properties. For instance, Jeong et al. proposed N-doped graphene as high-performance ultracapacitors, and Li et al. showed that some N defects make graphene nanoribbons into half-metals or spin gapless semiconductors [20–21]. However above all, doped N atoms can improve metal binding to the substrate due to their high chemical reactivity. Using this property, there have been various attempts to apply N-doped graphene to catalyst support for an oxygen reduction reaction or a hydrogen storage platform with metal treatment [22–23]. In addition, instead of chemical vapor deposition (CVD) technique, which was commonly used to manufacture N-doped graphene, new methods using chemical reactions have been recently reported to facilitate synthesize under mild conditions [24–25]. Thus, it is expected that N doping will be highly effective to promote further development of metal–graphene complex for applications in diverse fields without metal clustering.

In this paper, systematic studies on the interaction of metal adatom and N-doped graphene are presented. Previous theoretical work has demonstrated that bonding character between the metal and graphene is different according to the type of metal, and this difference affects the resultant binding energy [26]. In this perspective, the type

---

* Corresponding author. Fax: +82 2 2281 5308.
*E-mail address:* yongchae@hanyang.ac.kr (Y.-C. Chung).

0022-4596/$ - see front matter © 2013 Elsevier Inc. All rights reserved.
http://dx.doi.org/10.1016/j.jssc.2013.07.022

of N defects as well as that of metal can also change the bonding character of the metal on the substrate layer. Therefore, using density functional theory (DFT) based first-principles calculations, the effects of N defects on the bonding character and binding energy between the metal and graphene were investigated. Here, three types of N-doped graphene structures (graphitic, pyridinic, and pyrrolic) which are known as experimentally realizable were employed [24,27–28], and Li and Ti were chosen since these represent the metals which commonly preferred ionic and covalent bonding on the graphene, respectively [26].

## 2. Calculation method

DFT calculations [29] were performed using the Vienna ab initio simulation package (VASP) code [30]. Projector-augmented waves (PAW) [31] were used to describe the ion cores, and the exchange-correlation interactions were expressed with a generalized gradient approximation (GGA) in the form of the Perdew, Burke, and Ernzerhof (PBE) functional [29]. Here, the effect of van der Waals (vdW) interactions was included explicitly by using the empirical correction scheme of Grimme′s DFT-D2 method [32], as implemented by Bucko et al. for periodic systems [33]. The plane-wave basis set was expanded to a cutoff energy level of 500 eV. All of the self-consistent loops were iterated until the total energy difference of the systems between the adjacent iterating steps was less than $10^{-5}$ eV. The calculations were performed with a Γ-point centered $4\times4\times1$ k-point generated by the Monkhorst–Pack scheme [34]. The effective range of the cutoff energy and the validity of the mesh density used in this calculation were determined by a convergence test using the theoretically estimated lattice constants of pristine graphene, 2.464 Å. For the density of states, a Gaussian broadening scheme with a width of 0.02 eV was employed. Ionic relaxation was executed with the conjugate gradient method. The constituent atoms in metal decorated N-doped graphene systems were fully relaxed until the maximum Hellmann–Feynman forces were in the range of $\pm 0.01$ eV/Å. To simulate N-doped graphene structures, the supercell of a $4\times4$ hexagonal single layer of graphene was used. The graphene sheet was basically composed of 32 carbon atoms, and nitrogen atoms were suitably doped for each structure, as described in Fig. 1. The constructed supercells were periodically repeated with a 12 Å vacuum spacer lying vertically.

## 3. Results and discussion

To study the effect of N defects on the binding results between the metal and graphene, pristine graphene and three different defect models of N-doped graphene were employed, as shown in Fig. 1. A graphitic defect was constructed simply by substituting nitrogen atom for carbon atom. The formation of C–N bonds in this structure is similar to that in hybrid graphene/boron nitride (C–BN) monolayer which has been noticed due to its novel electronic and magnetic properties [35–37]. Thus, it is supposed that bonding character of graphitic defect with metal adatoms is also analogous to that of C–BN system. On the other hand, the pyridinic and pyrrolic defects were obtained by removing a carbon atom and replacing the three nearest carbon atoms with nitrogen atoms. The pyridinic defect is composed of only pyridinic nitrogen atoms, but the pyrrolic defect includes two pyridinic nitrogen atoms and one pyrrolic nitrogen atom that form a five-membered ring. For these N-doped graphene layers, the Li and Ti metals were dispersed on each defect. To find the most stable configuration of metal decoration, energetic comparison for the possible adsorption sites was performed. Of these adsorption sites considered, the site with the largest adsorption energy was referred to as the favored site. Fig. 1 shows the optimized adsorption geometry of Li metal on the N-doped graphene, and the corresponding adsorption position of the Ti adatom on the respective N defects is almost the same as the case of the Li adatom.

After being fully relaxed, the detailed binding results were investigated. In Table 1, the calculated binding energy ($E_b$) of a single metal on each type of layer was listed with the cohesive energy ($E_c$) of the metal bulk for comparison purposes. These $E_b$ values were derived as

$$E_b = E_M + E_{sub} - E_{M+sub}, \tag{1}$$

where $E_M$, $E_{sub}$, and $E_{M+sub}$ represent the energies of the isolated metal atom, the substrate (N-doped graphene sheet), and the metal dispersed N-doped graphene system, respectively. Additionally, the adatom height ($h$) and layer distortion ($d_{GC}$) were included in Table 1 to compare the adsorption geometry quantitatively. It is interesting to note that the $E_b$ of Ti for graphitic structure is almost

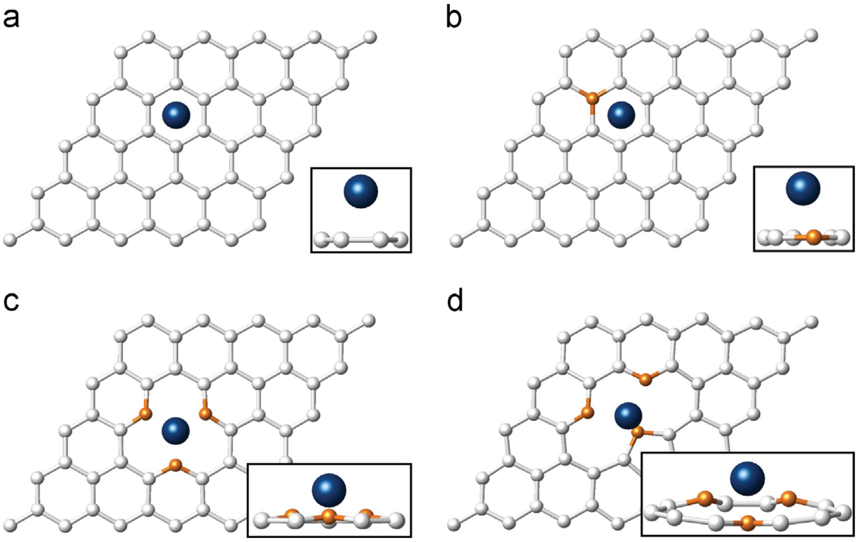

**Fig. 1.** The optimized geometries of Li decorated N-doped graphene (Top view): (a) pristine, (b) graphitic, (c) pyridinic, and (d) pyrrolic. White, orange, and blue balls represent carbon, nitrogen, and lithium atoms, respectively. (The side view of each system was presented in inset for clear understanding.) (For interpretation of the references to color in this figure legend, the reader is referred to the web version of this article.)